iScience

CellPress
OPEN ACCESS

Article

TBX15 facilitates malignant progression of glioma by transcriptional activation of TXDNC5

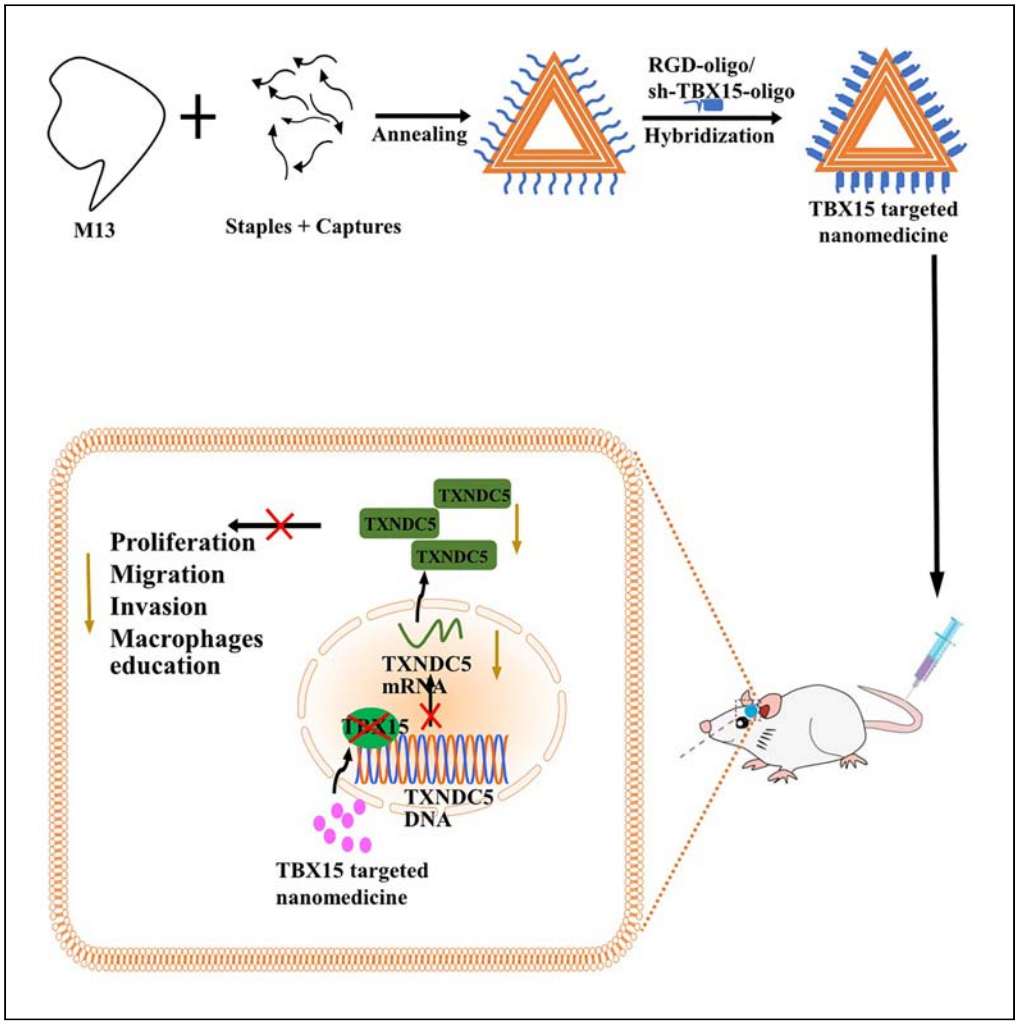

Yuyuan Ge, Bin Jia, Peng Zhang, ..., Yandong Xie, Zhe Li, Jun Dong

dongjun@suda.edu.cn

Highlights

TBX15 was elevated in glioma tissues and correlated to poor prognosis

TBX15 promoted the malignant phenotype of glioma

TBX15 facilitates glioma progression in a TXNDC5-dependent manner

shRNA-TBX15 assembled into DNA origami function as nanomedicine for glioma

Ge et al., iScience *27*, 108950
February 16, 2024
https://doi.org/10.1016/j.isci.2024.108950

iScience

CellPress
OPEN ACCESS

Article

TBX15 facilitates malignant progression of glioma by transcriptional activation of TXDNC5

Yuyuan Ge,[1,6] Bin Jia,[2,6] Peng Zhang,[3,4,6] Baomin Chen,[1] Liang Liu,[5] Yan Shi,[1] Shilu Huang,[1] Xinglei Liu,[1] Ran Wang,[5] Yandong Xie,[5] Zhe Li,[2] and Jun Dong[1,7,*]

SUMMARY

T-box transcription factor 15 (TBX15) plays important role in various cancers; however, its expression and role in glioma is still unclear. In this study, our findings indicated that TBX15 was increased in gliomas compared to normal brain tissues, and high levels of TBX15 were related to poor survival. Furthermore, TBX15 silencing in glioma cells not only inhibited their proliferation, migration, and invasion *in vitro*, but also weakened their ability to recruit macrophages and polarize the latter to the M2 subtype. Mechanism study indicated that thioredoxin domain containing 5 (TXNDC5) lies downstream of TBX15. Furthermore, rescue assays verified that the role of TBX15 in glioma cells is dependent on TXNDC5. Moreover, sh-TBX15 loaded into DNA origami nanocarrier suppressed the malignant phenotype of glioma *in vitro* and *in vivo*. Taken together, the TBX15/TXNDC5 axis is involved in the genesis and progression of glioma, and is a potential therapeutic target.

INTRODUCTION

Gliomas are a type of cancerous tumor that commonly occur in the central nervous system and are considered the most common form of primary brain tumors of adults.[1,2] Its characteristics include a high degree of malignancy, rapid development, and broad invasive growth.[3] Despite advances in treatment strategies, the combination of surgical resection and targeted radiotherapy/chemotherapy can improve the overall survival of low-grade glioma to a certain extent; however, the prognosis of high-grade glioma remains exceedingly poor.[4] Hence, it is important to elucidate the molecular mechanisms and signal pathways underlying glioma genesis and progression in order to identify novel therapeutic targets.

The family of T-box transcription factors (TBXs) has an important function in growth and development, such as differentiation of mesoderm, and the formation of heart and limbs.[5,6] Recent studies have shown that the TBXs are differentially expressed in many tumor tissues. TBX15, one important member of TBXs, is indispensable for skeletal differentiation and development.[7] In addition, TBX15 is also involved in the progression of esophageal cancer, pancreatic cancer, and ovarian cancer.[8–10] However, its role in glioma genesis and the underlying mechanisms remain unreported so far.

Thioredoxin domain containing 5 (TXNDC5) belongs to the family of protein disulfide isomerases (PDIs), and are mainly distributed in the endoplasmic reticulum and cell membrane.[11] Existing studies have shown that TXNDC5 is closely related to various biological phenotypes such as cell proliferation, migration and apoptosis.[12] In cancer research, TXNDC5 is upregulated in various tumor tissues and shows the function of an oncogene.[13,14] There is evidence that TXNDC5 is associated with the molecular characteristics of gliomas,[15] however, no potential molecular mechanisms have been clarified.

DNA origami is a unique self-assembly technology using a long, single-stranded DNA scaffold (usually phage M13), which is paired with numerous complementary short strands of DNA (usually 20 to 60 base pairs in length) that are programmed to fold into nanostructures of different shape and sizes.[16,17] Given its precise and controllable structure, easy chemical modification, and biodegradability, DNA origami has broad application prospects in biomolecular detection, targeted drug delivery and biomaterial synthesis. It is a suitable nanocarrier for transporting biomacromolecules, antisense oligonucleotide (ASO), short hairpin RNA (shRNA) and other molecules to tumor cells,[18] although the therapeutic potential of DNA origami against glioma has not been explored so far.

Our findings indicated that TBX15 was increased in the glioma tissues, and high levels of TBX15 were related to poor survival. Furthermore, our findings indicated that TBX15 exerts its oncogenic effects by activating its downstream target gene TXNDC5. A DNA origami-based

[1]Department of Neurosurgery, Second Affiliated Hospital of Soochow University, Suzhou 215004, China
[2]Department of Biomedical Engineering, College of Engineering and Applied Sciences, Nanjing University, Nanjing 210023, China
[3]Department of Neurosurgery, People's Hospital of Rugao, Nantong 226500, China
[4]Department of Neurosurgery, Rugao Clinical College, Jiangsu Health Vocational College, Nantong 226500, China
[5]Department of Neurosurgery, Affiliated Nanjing Brain Hospital, Nanjing Medical University, Nanjing 210029, China
[6]These authors contributed equally
[7]Lead contact
*Correspondence: dongjun@suda.edu.cn
https://doi.org/10.1016/j.isci.2024.108950

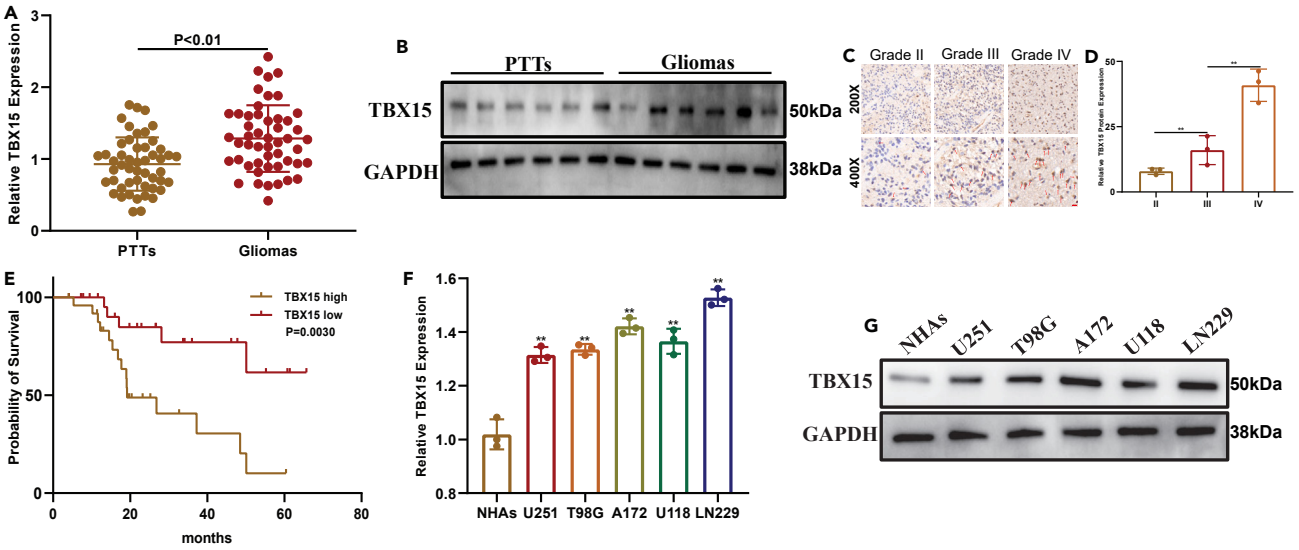

Figure 1. TBX15 was elevated in glioma tissues and correlated to poor prognosis

(A and B) TBX15 mRNA and protein expression among glioma and paired non-tumor tissues.

(C and D) Expression of TBX15 among glioma tissues as detected by immunohistochemistry. Scale bar, 20 μm.

(E) Kaplan-Meier survival curves of glioma patients demarcated on the basis of TBX15 expression.

(F and G) TBX15 mRNA and protein expression in indicated glioma cell lines was detected by qRT-PCR and western blot.

PTTs: paired peri-tumor tissues; TBX15: T-box transcription factor 15.

Data are represented as means ± SD. Statistical analysis of the data from two groups was performed using Student's *t* test. (**p < 0.01).

nanocarrier was constructed to transport sh-TBX15 to glioma cells, which effectively inhibited glioma growth. Collectively, TBX15/TXNDC5 axis plays important role in glioma, and has potential to become a therapeutic target.

RESULTS

TBX15 was elevated in glioma tissues and correlated to poor prognosis

We analyzed the relation between TBX15 level and clinical characteristics of glioma in The Cancer Genome Atlas (TCGA) and Chinese Glioma Genome Atlas (CGGA) cohorts. TBX15 expression was closely related to the age/grade/IDH mutation status of the glioma patients (Figures S1A, S1B, S2A, and S2B). Furthermore, glioma patients with higher TBX15 expression showed worse survival (Figures S1C and S2C). To verify these results, we collected clinical specimens and analyzed TBX15 mRNA and protein expression in the glioma and peri-tumor tissue (PTT) samples which indicated that TBX15 was increased in the gliomas tissues (Figures 1A–1D). The patients were divided into the $TBX15^{high}$ and $TBX15^{low}$ groups. As shown in Figure 1E, compared to the $TBX15^{low}$ group, the $TBX15^{high}$ group displayed a significantly shorter survival time. In addition, TBX15 was also increased in glioma cell lines compared to the normal astrocytes (Figures 1F and 1G). In sum, our results suggested that TBX15 was increased in gliomas and correlated with worse prognosis.

TBX15 promoted the malignant phenotype of glioma cells *in vitro*

To explore the oncogenic function of TBX15 in glioma, we transfected the A172 and LN229 cell lines with sh-TBX15, TBX15 overexpression plasmid and the respective controls. Verification of transfection efficiency was carried out through quantitative reverse transcription-polymerase chain reaction (qRT-PCR) together with western blotting (Figures 2A–2D). EdU assay showed that TBX15 knockdown inhibited glioma cell proliferation, while overexpression of TBX15 had the opposite effect (Figures 2E and 2F). Transwell assay showed that TBX15 promotes the migratory and invasive capacity of glioma cells (Figures 2G and 2H).

Tumor associated macrophages (TAMs), the most abundant cell type in glioma tissues apart from parenchyma cells, play an important role in the malignant progression of glioma.[19] Immune infiltration analysis was conducted using TCGA as well as CGGA data, which showed significantly greater infiltration of M2 macrophages in the $TBX15^{high}$ glioma tissues compared to the those with low TBX15 expression (Figures 3A and 3B). To investigate the potential involvement of TBX15 in TAM polarization, we induced THP-1 cells with phorbol 12-myristate 13-acetate (PMA) to differentiate them into macrophages and co-cultured the latter with glioma cells in transwell chambers. The co-culture assay showed that glioma cells expressing higher levels of TBX15 recruited more macrophages compared to those with lower TBX15 expression (Figures 3C and 3D). Moreover, the $TBX15^{high}$ glioma cells effectively polarized the macrophages toward the M2 phenotype compared to the $TBX15^{low}$ cells (Figures 3E and 3F). Based on these findings, it could be inferred that TBX15 promotes

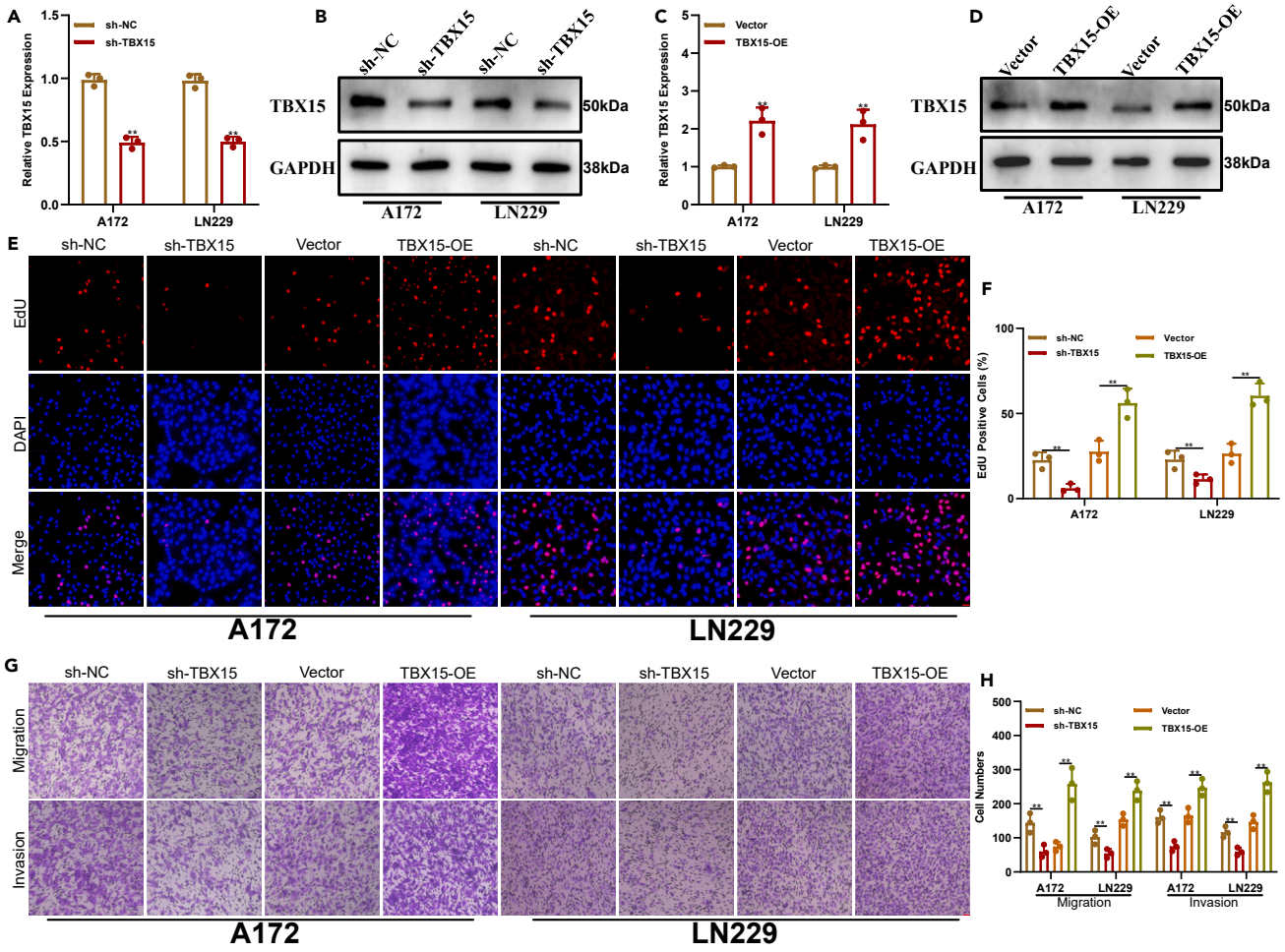

Figure 2. TBX15 promoted proliferation, migration, and invasion of glioma cells *in vitro*

(A–D) TBX15 mRNA and protein expression in glioma cell lines which transfected with sh-NC, sh-TBX15, vector or TBX15 overexpression plasmid, respectively.

(E–F) Evaluation of proliferative capacity of the indicated glioma cells using EdU assay. Scale bar, 20 μm.

(G–H) Assessment of migration and invasion ability of the indicated glioma cells using transwell assay. Scale bar, 100 μm.

Data are represented as means ± SD. Statistical analysis of the data from two groups was performed using Student's *t* test. (**p < 0.01).

the proliferation, migration, and invasion of glioma cells; besides, it also enhances their ability to recruit and polarize macrophages to the M2 phenotype.

TBX15 knockdown inhibited the growth of gliomas *in vivo*

LN229-Luci cells transfected with either sh-NC or sh-TBX15 were transplanted into the caudate nucleus of nude mice to construct glioma model *in vivo*. The tumorigenicity of the LN229 cells with TBX15 knockdown was significantly lower compared to that in the control group (Figures 4A and 4B), which corresponded to shorter overall survival in the latter (Figure 4C). The tumors were harvested after euthanizing the mice, and TBX15 expression was lower in the sh-TBX15 group compared to that in the control group (Figures 4D and 4E). Furthermore, the percentage of F4/80 positive cells was significantly lower in the sh-TBX15 tumors (Figures 4F and 4G). These results demonstrated that TBX15 promotes the growth of gliomas as well as the recruitment of macrophages *in vivo*.

TBX15 directly binds to promoter of TXNDC5 and promotes TXNDC5 expression in glioma cells

To clarify the mechanism underlying the role of TBX15 in glioma progression, we analyzed the transcriptomes of the control and TBX15-knockdown LN229 cells. As shown in Figure 5A, a total of 2,528 genes were dysregulated, of which 1,406 were downregulated and 1,122 upregulated in the TBX15-knockdown cells. We preliminarily screened ten genes for upregulation and ten genes for downregulation, respectively. Based on TCGA/CCGA analysis, their correlation with TBX15 was analyzed, and the results showed that compared with the upregulated genes, these downregulated genes had a higher correlation with TBX15. Given the reasons for the appeal, we chose the downregulated

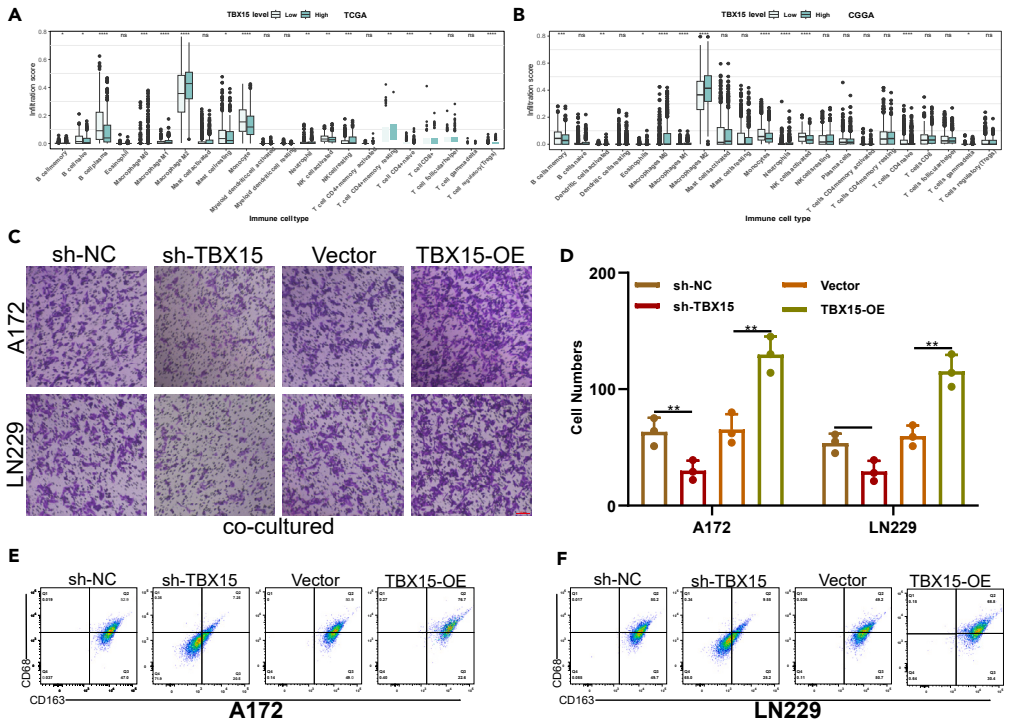

Figure 3. TBX15 promoted M2 polarization of macrophages by glioma cells

(A and B) Boxplots showing immune cell infiltration score in TBX15^{low} and TBX15^{high} groups in TCGA and CGGA cohorts.

(C and D) A co-culture model based on transwell insert was constructed for evaluating the ability of glioma cells to recruit macrophages. Scale bar, 100 μm.

(E and F) TAMs polarized by the glioma cells were measured by flow cytometry. The data about immunoinfiltration was analyzed by CIBERSORTx algorithm. Data are represented as means ± SD. Statistical analysis of the data from two groups was performed using Student's *t* test. (*p < 0.05, **p < 0.01, ***p < 0.001, ****p < 0.0001 ns: no significance).

genes to investigate and found that TXNDC5 was most significantly correlated with TBX15 in TCGA and CGGA datasets (Figures 5B and 5C; Figures S3 and S4). Furthermore, immune infiltration analysis based on TCGA and CGGA showed significant M2 macrophages infiltration in glioma tissues with high TXNDC5 expression compared to those with low TXNDC5 levels (Figures 5D and 5E; Figures S5 and S6). These findings indicated that TXNDC5 may function as a downstream target of TBX15.

To confirm our hypothesis, we conducted an analysis of the correlation of TXNDC5 expression levels with clinical characteristic of glioma patients included in TCGA and CGGA datasets, and found that TXNDC5 was closely related with the age/grade/IDH mutation/overall survival of glioma patients (Figure S7 and S8). Furthermore, TXNDC5 was highly expressed in glioma tissues and cells as well (Figure S9), and correlated positively with the expression of TBX15 (Figures 5F and 5G). Since TBX15 is a transcription factor, we surmised that TBX15 may exert its function by binding to the promoter region of TXNDC5, and promoting its transcription and translation. Therefore, we predicted the possible binding sites between TBX15 and TXNDC5 in the JASPAR and University of Colombo School of Computing (UCSC) databases, and identified three potential sites with high scores (Figures 5H and 5I). Vectors containing wild type/mutated TBX15 binding sequences were transfected into TBX15-overexpressing glioma cells. Luciferase reporter assay showed that TBX15 upregulation increased luciferase activity with the wild type and P2 constructs, whereas the P1 and P3 binding sites diminished the luciferase activity (Figures 5J and 5K), which suggested that TBX15 binds to the P2 region (56–63) of the TXNDC5 promoter. In addition, compared to the control group, silencing of TBX15 led to a decrease in the enrichment of TXNDC5 (Figures 5L and 5M). Moreover, ChIP assay and electrophoretic mobility shift assay (EMSA) assay confirmed that TBX15 interacted with the promoter sequence of TXNDC5 (Figures 5N–5P). Taken together, these findings suggested that TBX15 attaches to the promoter of TXNDC5, thereby regulating its gene expression.

TBX15 facilitates glioma progression in a TXNDC5-dependent manner

To further ascertain whether TBX15 exerts its oncogenic effects via TXNDC5, we performed rescue experiments. Ectopic expression of TXNDC5 partially offset the downregulation of TXNDC5 caused by TBX15 knockdown (Figures 6A–6D). Furthermore, TXNDC5 upregulation neutralized the inhibitory role of sh-TBX15 in the proliferation (Figures 6E and 6F), migration, as well as invasion (Figures 6G and 6H) of glioma cells. In addition, TXNDC5 also restored the ability of the TBX15-knockdown glioma cells to recruit macrophages, and enhanced the M2 polarization of the latter (Figures 6I–6K). Taken together, TBX15 facilitates the malignant progression of glioma in a TXNDC5-dependent manner.

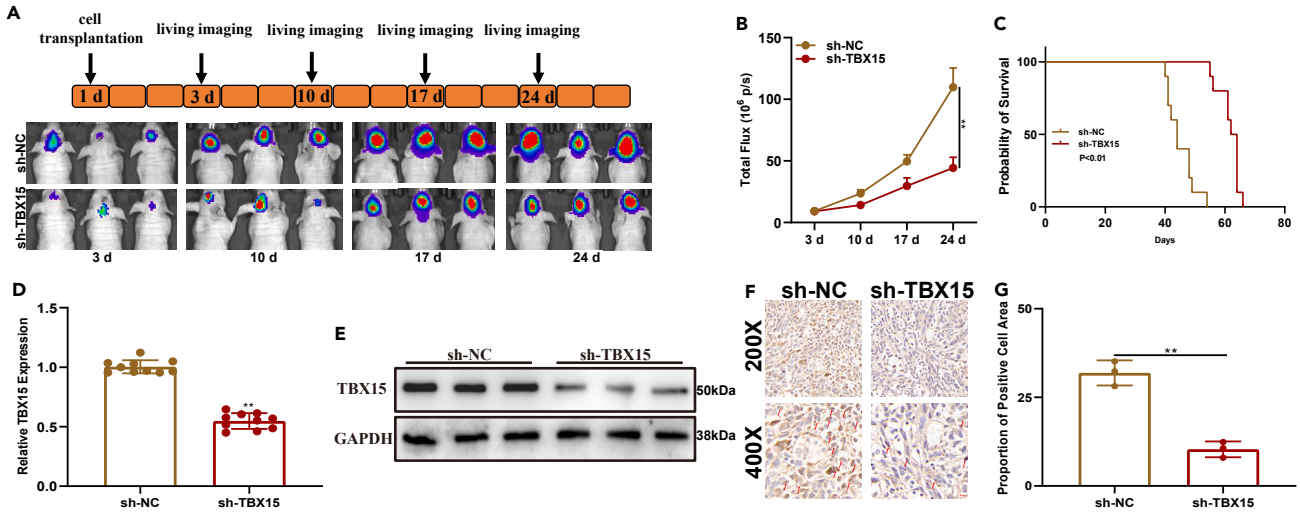

Figure 4. TBX15 knockdown inhibited the growth of gliomas *in vivo*

(A and B) Representative images of tumor growth at the indicated time points detected by living imaging analysis.

(C) Kaplan-Meier survival curves of the tumor bearing mice.

(D and E) TBX15 mRNA and protein levels in tumors from the indicated groups.

(F and G) F4/80-positive cells among the tumors from the indicated groups were detected by immunohistochemistry. Scale bar, 20 μm.

Data are represented as means ± SD. Statistical analysis of the data from two groups was performed using Student's *t* test. (**p < 0.01).

shRNA-TBX15 assembled into DNA origami function as nanomedicine for glioma targeted therapy

In a previous study, we found that DNA origami loaded with folic acid effectively treated rheumatoid arthritis.[20] We assembled sh-TBX15 into DNA origami, and decorated the nanoparticles with RGD peptides to target glioma cells. Atomic force microscope and dynamic light scattering were adopted to analyze the morphology and size of the nanoparticles, respectively (Figure S10A). The DNA origami significantly enhanced the phagocytosis of sh-TBX15 into the glioma cells (Figures S10B and S10C), and subsequently amplified sh-TBX15's inhibitory impact on the proliferation, migration and invasion of glioma cells, as well as the recruitment and polarization of macrophages (Figures S10D–S10J).

To evaluate the therapeutic ability of the nanoparticles *in vivo*, we established an intracranial orthotopic tumor model in nude mice and injected the DNA origami complex through the tail vein. The DNA origami loaded with sh-TBX15 effectively inhibited glioma growth (Figures 7A and 7B) and improved overall survival of the tumor-bearing mice (Figure 7C). The tumor tissues from mice treated with sh-TBX15 nanoparticles expressed significantly lower levels of TBX15 and TXNDC5 compared to that in the control group (Figures 7D and 7E), and also showed a marked decreased in the percentage of F4/80 positive cells (Figures 7F and 7G). Furthermore, we also confirmed that the nanoparticles accumulated selectively in the glioma tissues (Figure S11A). H&E staining of the major organs did not indicate any significant tissue damage due the DNA origami nanoparticles (Figure S11B). Taken together, shRNA-TBX15 assembled into DNA origami can safely and effectively inhibit glioma growth.

DISCUSSION

Glioma is a significant burden to health due to its high malignancy and mortality. In addition to surgery, radiotherapy and chemotherapy, targeted therapy is a promising option for treating glioma. Identifying the key factors involved in glioma progression is crucial for developing new targeted therapeutic strategies.

The TBX family is evolutionarily conserved and consists of the Brachyury (T), T-Brain (Tbr1), TBX1, TBX2, and TBX6 sub-families.[21] The TBX family is ubiquitously expressed and has important function in early cell fate determination and organ formation. In addition, the TBX proteins function as oncogenes and/or tumor suppressors in various cancers. For instance, Zhao et al. have found the upregulation of TBX15 in lung cancer, which subsequently activates TNFSF11 transcription and promotes carcinogenic progression.[22] As reported by Jiang et al., TBX15 could promote miR-152's transcription to enhance the sensitivity of breast cancer cells to doxorubicin, and miR-152 further inhibits the expression of kinesin family member 2C (KIF2C).[23] Xie et al. showed that clear cell renal cell carcinoma samples exhibited increased levels of TBX15, which correlated with worse outcome.[24] There is a study showed that TBX15 was upregulated in glioma tissues and indicated poor prognosis of glioma patients.[25] Results of our study on gliomas was consistent with these studies. In addition, knocking down TBX15 in glioma cells repressed their proliferation, migration and invasion rates, along with their ability to polarize macrophages to the M2 phenotype. Our study suggested a close correlation between TBX15 and glioma progression, highlighting its potential as a promising therapeutic target.

At the molecular level, we were able to verify that TBX15 binds to the 56–63 region of the TXNDC5 promoter. TXNDC5, an important member of the thioredoxin family, is involved in protein folding and functions as a molecular chaperone.[26] Thioredoxin promotes the formation of

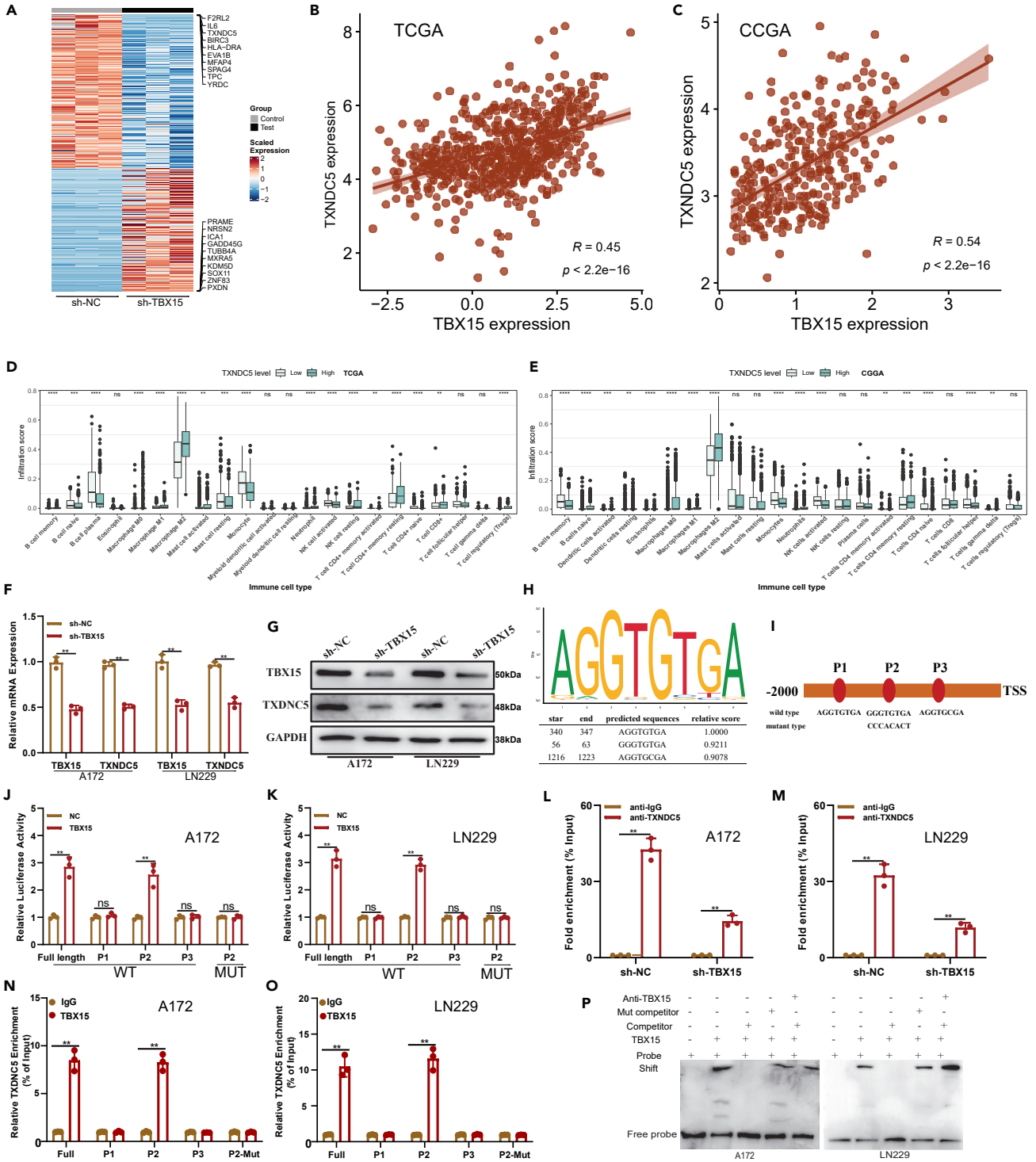

Figure 5. TBX15 directly binds to the promoter of TXNDC5 and activates transcription in glioma cells

(A) Differentially expressed genes between the A172 cells transfected with sh-NC and sh-TBX15 were analyzed by RNA sequencing.

(B and C) Correlation between TBX15 and TXNDC5 in glioma tissues based on TCGA and CGGA data was analyzed by Pearson's correlation.

(D and E) Boxplots showing immune cell infiltration score in TXNDC5^{high} and TXNDC5^{low} groups based on TCGA and CGGA data.

(F and G) Expression of TBX15/TXNDC5 in A172 and LN229 cells transfected with sh-NC and sh-TBX15 was detected by qRT-PCR and western blot, respectively.

(H) TBX15 potentially binds to the promoter region of TXNDC5 according to data form JASPAR.

(I) The schematic illustration of wild type and mutated binding sites for TBX15 in the luciferase reporter vector.

Figure 5. *Continued*

(J and K) TBX15 upregulation increased luciferase activity with the wild type and P2 constructs, whereas the P1 and P3 binding sites diminished the luciferase activity.

(L and M) TXNDC5 enrichment in the immunoprecipitants of IgG or anti-TXNDC5 antibody.

(N and O) ChIP assay showed that TXDNC5 promoter was enriched in anti-TBX15 group.

(P) EMSA assay confirmed that TBX15 interacted with the promoter sequence of TXNDC5.

Data are represented as means ± SD. Statistical analysis of the data from two groups was performed using Student's *t* test. Correlation scatterplot of the data was performed using Pearson's correlation coefficient. The data about immunoinfiltration was analyzed by CIBERSORTx algorithm. (*p < 0.05, **p < 0.01, ***p < 0.001, ****p < 0.0001, ns: no significance).

disulfide bonds in target proteins and regulates intracellular oxidation-reduction reaction. Several members of the thioredoxin family are increased in tumor tissues and involved in abnormal proliferation of tumor cells. TXDNC5 is increased in multiple tumors, including lung, colon, cervical, and hepatocellular cancers. Pei et al. reported that TXNDC5 is a target of METTL3-mediated m6A modification and mediates progression of cervical cancer.[13] The study of Xia et al. suggested that TXNDC5 may regulate the progression of esophageal cancer through the PI3K/AKT pathway.[14] Additionally, two studies have found that TXDNC5 was upregulated among the tissues of liver cancer as well as gliomas, and it is associated with poor prognosis in glioma.[15,27] Our findings are consistent and indicate that TXNDC5 is a potential prognostic marker for glioma. Moreover, functional assays showed that TXNDC5 neutralized the inhibitory effect of TBX15 knockdown on the malignant phenotype of glioma. Our study suggested that TBX15 enhanced glioma progression by upregulating TXNDC5. Previous research has demonstrated that TXNDC5 plays a significant role in the advancement of prostate cancer by interacting with the androgen receptor.[12] Additionally, it has been found to regulate the expression of SERPINF1/TRAF1, thereby influencing the expression of cervical cancer. Furthermore, TXNDC5 has the ability to modulate the sensitivity of AKT, ERK1/2, EMT, and HER2 signaling pathways under hypoxic conditions.[12] These findings suggest that the aforementioned signaling pathways may serve as downstream regulatory targets of TBX15/TXNDC5. However, further investigation is required to fully comprehend the involvement of these signaling axes in glioma progression.

With the development of gene editing, gene silencing and other gene manipulation techniques, site-specific upregulation or downregulation of target gene is rapidly emerging as a promising strategy to treat various diseases, especially cancers.[28,29] Small molecule drugs exhibit instability in the blood and poor cellular absorption, therefore, delivery vectors are needed to increase the anti-cancer efficacy. DNA origami, a two-dimensional or three-dimensional programmable nanostructure, can not only interact with small molecules, nucleic acids, proteins, viruses, and cancer cells, but also act as a nanocarrier to deliver different therapeutic drugs. Lee et al. established a DNA tetrahedron as a delivery vehicle, and achieved targeted gene silencing at the tumor site in nude mouse model.[30] The nanoparticles did not cause significant immune response, and their half-life in circulation was significantly longer than that of siRNA alone.[31] Liu et al. effectively loaded sgRNA/Cas9/antisense complex through DNA origami to achieve editing and silencing of tumor-promoting gene PLK1 (Polo-like kinase 1), thereby achieving excellent therapeutic results without serious adverse events.[32] In a previous study, we constructed a triangular DNA origami nanostructure (tDON) that was modified with folic acid, which effectively inhibited rheumatoid arthritis progression.[20] Likewise, we assembled sh-TBX15 into triangular DNA origami for targeted glioma therapy. The sh-TBX15 nanoparticles were stable and readily phagocytosed by glioma cells, and could selectively accumulate in the glioma tissues after crossing the blood-brain barrier and inhibit tumor growth.

In summary, TBX15 functions as an oncogene in glioma by promoting transcription and translation of TXNDC5. DNA origami loaded with sh-TBX15 can effectively inhibit progression of glioma (Figure 8). Therefore, TBX15 is a potential therapeutic target for glioma.

Limitation of the study

In present study, we found that TBX15 was increased in the glioma tissues, and high levels of TBX15 were related to poor survival. Furthermore, our findings indicated that TBX15 exerts its oncogenic effects by activating its downstream target gene TXNDC5. Based on this mechanism, we used nanocarriers to load sh-TBX5 and evaluated its efficacy in the treatment of glioma. However, evaluations on the pharmacokinetics of constructed nanomedicines are incomplete.

STAR★METHODS

Detailed methods are provided in the online version of this paper and include the following:

- KEY RESOURCES TABLE
- RESOURCE AVAILABILITY
  - Lead contact
  - Materials availability
  - Data and code availability
- EXPERIMENTAL MODEL AND STUDY PARTICIPANT DETAILS
  - Patients and specimens
  - Animal studies
  - Ethics approval and consent to participate
  - Consent for publication
- METHOD DETAILS

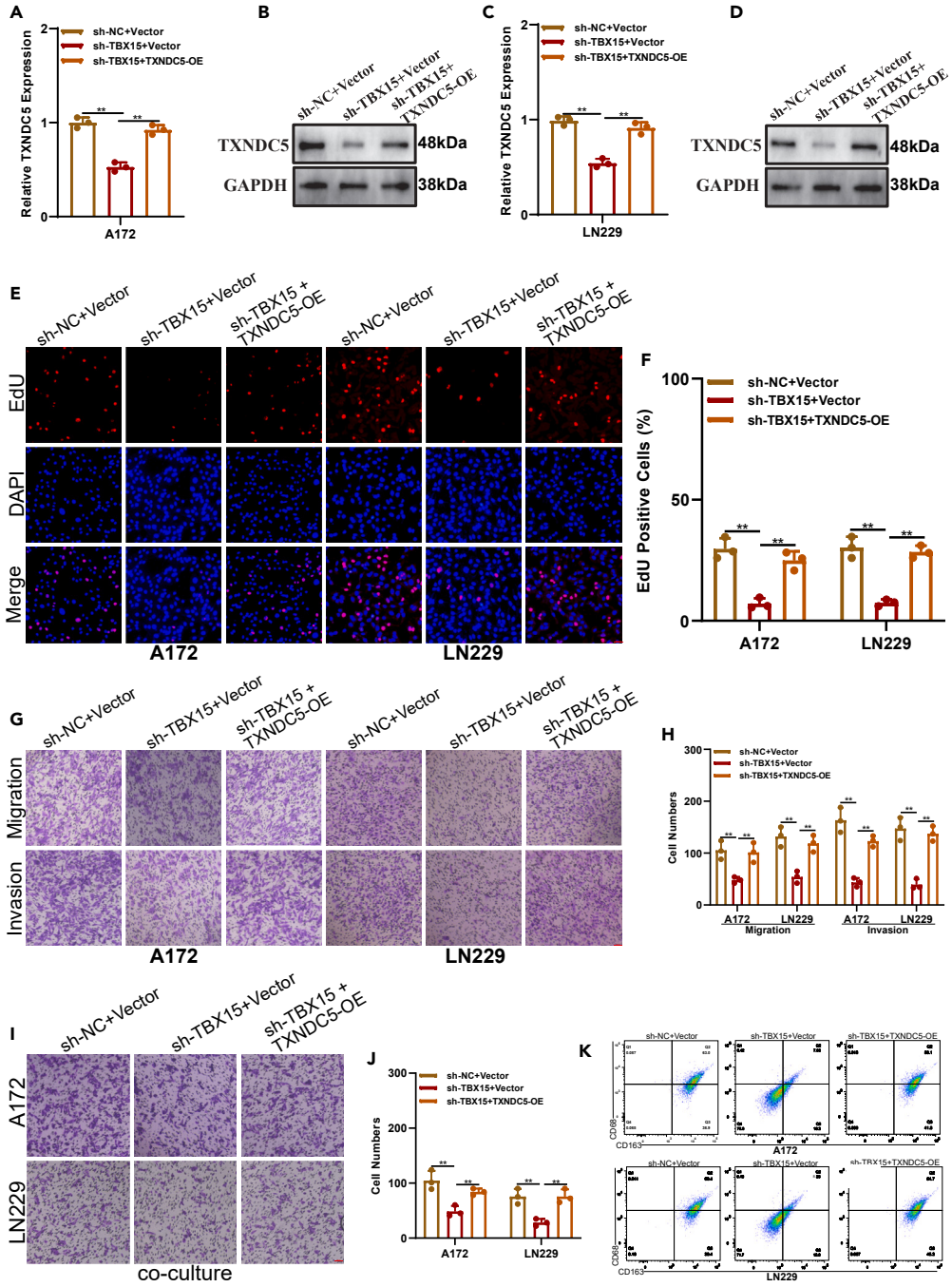

Figure 6. TBX15 facilitates malignant progression of glioma in a TXNDC5-dependent manner

(A–D) TXNDC5 mRNA and protein expression in glioma cell lines which transfected with sh-TBX15, sh-TBX15+TXNDC5-OE or corresponding negative control was detected by qRT-PCR and western blot.

(E and F) Proliferative capacity of the indicated glioma cells evaluated by EdU assay. Scale bar, 20 μm.

(G and H) Assessment of migration and invasion ability of the indicated glioma cells using transwell assay. Scale bar, 100 μm.

(I and J) Ability of the indicated glioma cells to recruit macrophages was evaluated by the co-culture model. Scale bar, 100 μm.

(K) TAMs polarized by the indicated glioma cells were evaluated by flow cytometry.

Data are represented as means ± SD. Statistical analysis of the data from two groups was performed using Student's *t* test. (**p < 0.01).

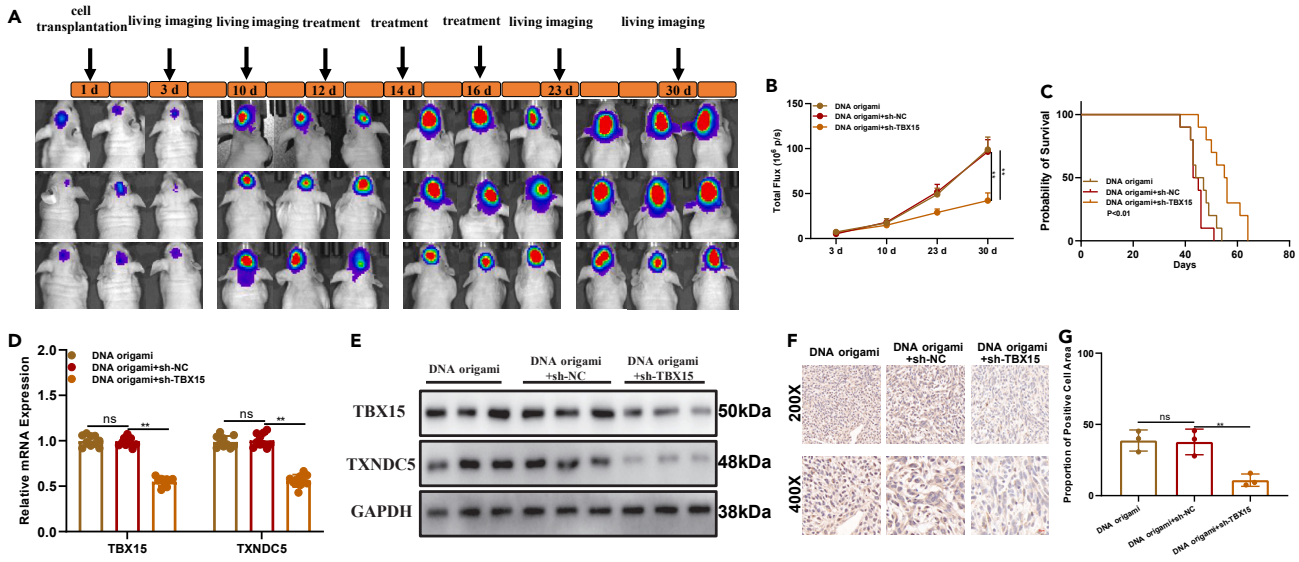

Figure 7. shRNA-TBX15 assembled into DNA origami for targeted glioma therapy

(A and B) Representative images captured by living imaging analysis showing tumor growth at the indicated time points.

(C) Kaplan-Meier survival curves of the tumor bearing mice.

(D and E) Expression of TBX15/TXNDC5 in the tumors from the indicated groups was detected by qRT-PCR and western blot.

(F and G) F4/80-positive cells among the tumors from the indicated groups were detected by immunohistochemistry. Scale bar, 20 μm.

Data are represented as means ± SD. Statistical analysis of the data from two groups was performed using Student's *t* test. (**p < 0.01, ns: no significance).

- Data collection
- Survival analysis
- Immune cell infiltration analysis
- Cell culture and transfection
- Quantitative reverse transcription-polymerase CHAIN reaction
- Western blotting
- EdU assay

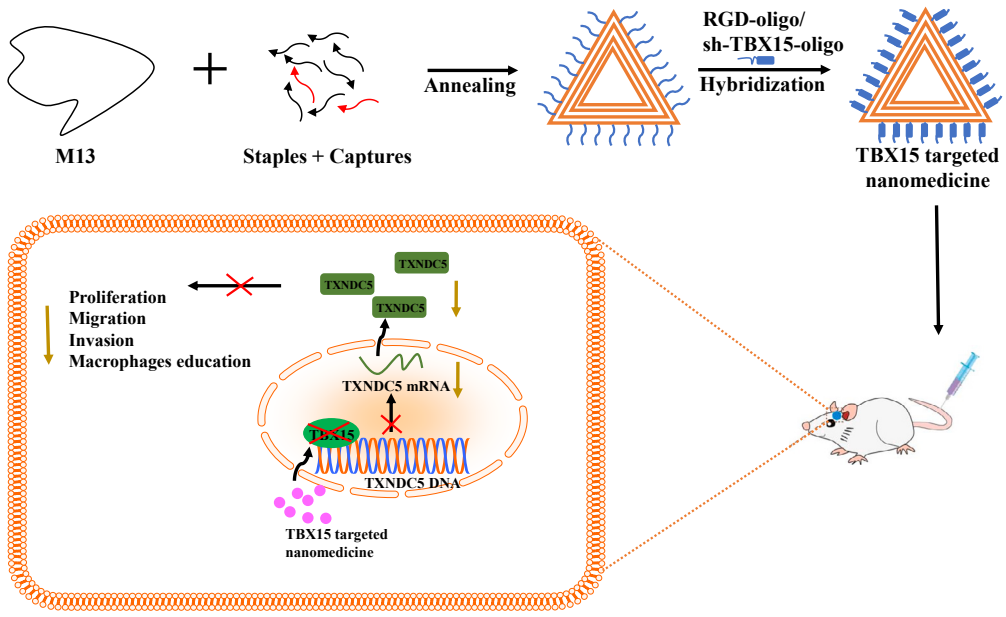

Figure 8. Working model of TBX15 facilitates malignant progression of glioma by transcriptional activation of TXDNC5

- Transwell assay
- Co-culture model
- Flow cytometry
- Luciferase reporter assay
- Immunohistochemistry (IHC)
- Synthesis of nanoplatform

- QUANTIFICATION AND STATISTICAL ANALYSIS

SUPPLEMENTAL INFORMATION

Supplemental information can be found online at https://doi.org/10.1016/j.isci.2024.108950.

ACKNOWLEDGMENTS

This study was supported by Jiangsu province key research and development program: Social development project (BE2021653), Key project of Jiangsu Health Commission (ZDB2020016), National Natural Science Foundation of China (82203637), Science and Technology Development Foundation of Nanjing Medical University (NMUB20210220). Scientific Research Project of Nantong Health Committee (MB2021086), Guidance project of Rugao Science and Technology Bureau (SRG (22)1068), and School-level scientific research project of Jiangsu Health Vocational College (JKC2022041).

AUTHOR CONTRIBUTIONS

J.D., L.L., and P.Z. designed and funded the study. Y.Y.G., B.J., and P.Z. performed this research and contributed equally to this study. B.J. and Z.L. conducted experiments on DNA origami. B.M.C., L.L., and Y.S. assisted with this research. S.L.H. and X.L.L. analyzed the data. R.W. and Y.D.X. performed bioinformatics analysis. Y.Y.G., B.J., P.Z., and L.L. wrote the manuscript. All authors approved the submitted version.

DECLARATION OF INTERESTS

The authors declare no competing interests.

Received: July 19, 2023
Revised: October 3, 2023
Accepted: January 15, 2024
Published: January 18, 2024

REFERENCES

1. Ratliff, M., Karimian-Jazi, K., Hoffmann, D.C., Rauschenbach, L., Simon, M., Hai, L., Mandelbaum, H., Schubert, M.C., Kessler, T., Uhlig, S., et al. (2023). Individual glioblastoma cells harbor both proliferative and invasive capabilities during tumor progression. Neuro Oncol. *25*, 2150–2162. https://doi.org/10.1093/neuonc/noad109.
2. Jiang, H., Zhu, Q., Wang, X., Li, M., Shen, S., Yang, C., Zhao, X., Li, M., Ma, G., Zhao, X., et al. (2023). Characterization and clinical implications of different malignant transformation patterns in diffuse low-grade gliomas. Cancer Sci. *114*, 3708–3718. https://doi.org/10.1111/cas.15889.
3. Kocakavuk, E., Johnson, K.C., Sabedot, T.S., Reinhardt, H.C., Noushmehr, H., and Verhaak, R.G.W. (2023). Hemizygous CDKN2A deletion confers worse survival outcomes in IDHmut-noncodel gliomas. Neuro Oncol. *25*, 1721–1723. https://doi.org/10.1093/neuonc/noad095.
4. Liu, L., Zhou, X., Cheng, S., Ge, Y., Chen, B., Shi, J., Li, H., Li, S., Li, Y., Yuan, J., et al. (2023). RNA-binding protein DHX9 promotes glioma growth and tumor-associated macrophages infiltration via TCF12. CNS Neurosci. Ther. *29*, 988–999. https://doi.org/10.1111/cns.14031.
5. Kimura, J.O., Bolaños, D.M., Ricci, L., and Srivastava, M. (2022). Embryonic origins of adult pluripotent stem cells. Cell *185*, 4756–4769.e13. https://doi.org/10.1016/j.cell.2022.11.008.
6. Ji, X., Chen, X., Zhang, B., Xie, M., Zhang, T., Luo, X., Liu, D., Feng, Y., Wang, Y., Sun, M., et al. (2022). T-box transcription factor 19 promotes hepatocellular carcinoma metastasis through upregulating EGFR and RAC1. Oncogene *41*, 2225–2238. https://doi.org/10.1038/s41388-022-02249-2.
7. Pan, D.Z., Miao, Z., Comenho, C., Rajkumar, S., Koka, A., Lee, S.H.T., Alvarez, M., Kaminska, D., Ko, A., Sinsheimer, J.S., et al. (2021). Identification of TBX15 as an adipose master trans regulator of abdominal obesity genes. Genome Med. *13*, 123. https://doi.org/10.1186/s13073-021-00939-2.
8. Qin, Y., Wu, C.W., Taylor, W.R., Sawas, T., Burger, K.N., Mahoney, D.W., Sun, Z., Yab, T.C., Lidgard, G.P., Allawi, H.T., et al. (2019). Discovery, Validation, and Application of Novel Methylated DNA Markers for Detection of Esophageal Cancer in Plasma. Clin. Cancer Res. *25*, 7396–7404. https://doi.org/10.1158/1078-0432.CCR-19-0740.
9. Majumder, S., Raimondo, M., Taylor, W.R., Yab, T.C., Berger, C.K., Dukek, B.A., Cao, X., Foote, P.H., Wu, C.W., Devens, M.E., et al. (2020). Methylated DNA in Pancreatic Juice Distinguishes Patients With Pancreatic Cancer From Controls. Clin. Gastroenterol. Hepatol. *18*, 676–683.e3. https://doi.org/10.1016/j.cgh.2019.07.017.
10. Wu, T.I., Huang, R.L., Su, P.H., Mao, S.P., Wu, C.H., and Lai, H.C. (2019). Ovarian cancer detection by DNA methylation in cervical scrapings. Clin. Epigenet. *11*, 166. https://doi.org/10.1186/s13148-019-0773-3.
11. Hung, C.T., Tsai, Y.W., Wu, Y.S., Yeh, C.F., and Yang, K.C. (2022). The novel role of ER protein TXNDC5 in the pathogenesis of organ fibrosis: mechanistic insights and therapeutic implications. J. Biomed. Sci. *29*, 63. https://doi.org/10.1186/s12929-022-00850-x.
12. Wang, X., Li, H., and Chang, X. (2022). The role and mechanism of TXNDC5 in diseases. Eur. J. Med. Res. *27*, 145. https://doi.org/10.1186/s40001-022-00770-4.
13. Du, Q.Y., Huo, F.C., Du, W.Q., Sun, X.L., Jiang, X., Zhang, L.S., and Pei, D.S. (2022). METTL3 potentiates progression of cervical cancer by suppressing ER stress via regulating m6A modification of TXNDC5 mRNA. Oncogene *41*, 4420–4432. https://doi.org/10.1038/s41388-022-02435-2.
14. Wang, H., Yang, X., Guo, Y., Shui, L., Li, S., Bai, Y., Liu, Y., Zeng, M., and Xia, J. (2019). HERG1 promotes esophageal squamous cell carcinoma growth and metastasis through TXNDC5 by activating the PI3K/AKT

pathway. J. Exp. Clin. Cancer Res. *38*, 324. https://doi.org/10.1186/s13046-019-1284-y.
15. Kocatürk, B. (2023). Identification of thioredoxin domain containing family members' expression pattern and prognostic value in diffuse gliomas via in silico analysis. Cancer Med. *12*, 3830–3844. https://doi.org/10.1002/cam4.5169.
16. Tang, Y., Liu, H., Wang, Q., Qi, X., Yu, L., Šulc, P., Zhang, F., Yan, H., and Jiang, S. (2023). DNA Origami Tessellations. J. Am. Chem. Soc. *145*, 13858–13868. https://doi.org/10.1021/jacs.3c03044.
17. Lu, Z., Liu, Y., Deng, Y., Jia, B., Ding, X., Zheng, P., and Li, Z. (2022). OaAEP1-mediated PNA-protein conjugation enables erasable imaging of membrane proteins. Chem. Commun. *58*, 8448–8451. https://doi.org/10.1039/d2cc02153f.
18. Pan, Q., Nie, C., Hu, Y., Yi, J., Liu, C., Zhang, J., He, M., He, M., Chen, T., and Chu, X. (2020). Aptamer-Functionalized DNA Origami for Targeted Codelivery of Antisense Oligonucleotides and Doxorubicin to Enhance Therapy in Drug-Resistant Cancer Cells. ACS Appl. Mater. Interfaces *12*, 400–409. https://doi.org/10.1021/acsami.9b20707.
19. Li, J., Wang, K., Yang, C., Zhu, K., Jiang, C., Wang, M., Zhou, Z., Tang, N., Wang, Q., Wang, S., et al. (2023). Tumor-Associated Macrophage-Derived Exosomal LINC01232 Induces the Immune Escape in Glioma by Decreasing Surface MHC-I Expression. Adv. Sci. *10*, e2207067. https://doi.org/10.1002/advs.202207067.
20. Ma, Y., Lu, Z., Jia, B., Shi, Y., Dong, J., Jiang, S., and Li, Z. (2022). DNA Origami as a Nanomedicine for Targeted Rheumatoid Arthritis Therapy through Reactive Oxygen Species and Nitric Oxide Scavenging. ACS Nano *16*, 12520–12531. https://doi.org/10.1021/acsnano.2c03991.
21. Karolak, J.A., Vincent, M., Deutsch, G., Gambin, T., Cogné, B., Pichon, O., Vetrini, F., Mefford, H.C., Dines, J.N., Golden-Grant, K., et al. (2019). Complex Compound Inheritance of Lethal Lung Developmental Disorders Due to Disruption of the TBX-FGF Pathway. Am. J. Hum. Genet. *104*, 213–228. https://doi.org/10.1016/j.ajhg.2018.12.010.
22. Li, P., Li, Y., Bai, S., Zhang, Y., and Zhao, L. (2023). miR-4732-3p prevents lung cancer progression via inhibition of the TBX15/TNFSF11 axis. Epigenomics *15*, 195–207. https://doi.org/10.2217/epi-2023-0009.
23. Jiang, C.F., Xie, Y.X., Qian, Y.C., Wang, M., Liu, L.Z., Shu, Y.Q., Bai, X.M., and Jiang, B.H. (2021). TBX15/miR-152/KIF2C pathway regulates breast cancer doxorubicin resistance via promoting PKM2 ubiquitination. Cancer Cell Int. *21*, 542. https://doi.org/10.1186/s12935-021-02235-w.
24. Zheng, Z., Chen, Z., Zhong, Q., Zhu, D., Xie, Y., Shangguan, W., and Xie, W. (2021). CircPVT1 promotes progression in clear cell renal cell carcinoma by sponging miR-145-5p and regulating TBX15 expression. Cancer Sci. *112*, 1443–1456. https://doi.org/10.1111/cas.14814.
25. Yan, D., Yu, Y., Ni, Q., Meng, Q., Wu, H., Ding, S., Liu, X., Tang, C., Liu, Q., and Yang, K. (2023). The overexpression and clinical significance of TBX15 in human gliomas. Sci. Rep. *13*, 9771. https://doi.org/10.1038/s41598-023-36410-y.
26. Shearn, C.T., Anderson, A.L., Miller, C.G., Noyd, R.C., Devereaux, M.W., Balasubramaniyan, N., Orlicky, D.J., Schmidt, E.E., and Sokol, R.J. (2023). Thioredoxin reductase 1 regulates hepatic inflammation and macrophage activation during acute cholestatic liver injury. Hepatol. Commun. *7*, e0020. https://doi.org/10.1097/HC9.0000000000000020.
27. Yu, J., Yang, M., Zhou, B., Luo, J., Zhang, Z., Zhang, W., and Yan, Z. (2019). CircRNA-104718 acts as competing endogenous RNA and promotes hepatocellular carcinoma progression through microRNA-218-5p/TXNDC5 signaling pathway. Clin. Sci. *133*, 1487–1503. https://doi.org/10.1042/CS20190394.
28. Yu, Y., Xu, B., Xiang, L., Ding, T., Wang, N., Yu, R., Gu, B., Gao, L., Maswikiti, E.P., Wang, Y., et al. (2023). Photodynamic therapy improves the outcome of immune checkpoint inhibitors via remodelling anti-tumour immunity in patients with gastric cancer. Gastric Cancer *26*, 798–813. https://doi.org/10.1007/s10120-023-01409-x.
29. Newald, J. (1986). Vital do's of case management. Hospitals *60*, 86.
30. Tian, T., Zhang, T., Shi, S., Gao, Y., Cai, X., and Lin, Y. (2023). A dynamic DNA tetrahedron framework for active targeting. Nat. Protoc. *18*, 1028–1055. https://doi.org/10.1038/s41596-022-00791-7.
31. Lee, H., Lytton-Jean, A.K.R., Chen, Y., Love, K.T., Park, A.I., Karagiannis, E.D., Sehgal, A., Querbes, W., Zurenko, C.S., Jayaraman, M., et al. (2012). Molecularly self-assembled nucleic acid nanoparticles for targeted in vivo siRNA delivery. Nat. Nanotechnol. *7*, 389–393. https://doi.org/10.1038/nnano.2012.73.
32. Liu, J., Wu, T., Lu, X., Wu, X., Liu, S., Zhao, S., Xu, X., and Ding, B. (2019). A Self-Assembled Platform Based on Branched DNA for sgRNA/Cas9/Antisense Delivery. J. Am. Chem. Soc. *141*, 19032–19037. https://doi.org/10.1021/jacs.9b09043.
33. Liu, L., Zhang, P., Dong, X., Li, H., Li, S., Cheng, S., Yuan, J., Yang, X., Qian, Z., and Dong, J. (2021). Circ_0001367 inhibits glioma proliferation, migration and invasion by sponging miR-431 and thus regulating NRXN3. Cell Death Dis. *12*, 536. https://doi.org/10.1038/s41419-021-03834-1.
34. Liu, L., Cui, S., Wan, T., Li, X., Tian, W., Zhang, R., Luo, L., and Shi, Y. (2018). Long non-coding RNA HOTAIR acts as a competing endogenous RNA to promote glioma progression by sponging miR-126-5p. J. Cell. Physiol. *233*, 6822–6831. https://doi.org/10.1002/jcp.26432.
35. Liu, L., Li, X., Wu, H., Tang, Y., Li, X., and Shi, Y. (2021). The COX10-AS1/miR-641/E2F6 Feedback Loop Is Involved in the Progression of Glioma. Front. Oncol. *11*, 648152. https://doi.org/10.3389/fonc.2021.648152.
36. Liu, L., Li, X., Shi, Y., and Chen, H. (2021). Long noncoding RNA DLGAP1-AS1 promotes the progression of glioma by regulating the miR-1297/EZH2 axis. Aging (Albany NY) *13*, 12129–12142. https://doi.org/10.18632/aging.202923.
37. Liu, L., Cui, S., Zhang, R., Shi, Y., and Luo, L. (2017). MiR-421 inhibits the malignant phenotype in glioma by directly targeting MEF2D. Am. J. Cancer Res. *7*, 857–868.

STAR★METHODS

KEY RESOURCES TABLE

REAGENT or RESOURCE	SOURCE	IDENTIFIER
Antibodies		
rabbit anti-TBX15 (WB)	Proteintech	Cat.25148-1-AP
rabbit anti-TXNDC5 (WB)	Proteintech	Cat.19834-1-AP
rabbit anti-GAPDH (WB)	Proteintech	Cat.60004-1-Ig
HRP-conjugated conjugated goat anti-mouse IgG	Proteintech	Cat.SA00001-1
HRP-conjugated conjugated goat anti-rabbit IgG	Proteintech	Cat.SA00001-2
rabbit anti-TBX15 (IHC)	Invitrogen	Cat.PA5-36143
rabbit anti-TXNDC5 (IHC)	Invitrogen	Cat.PA5-83240
anti-CD68 (FCM)	Biolegend	Cat.333813
anti-CD163 (FCM)	Biolegend	Cat.333605
Chemicals, peptides, and recombinant proteins		
DMSO	MedChemExpress	Cat.HY-100218A
RNAlater	Thermo Fisher	Cat.AM7020
RIPA lysis buffer	KeyGEN	Cat.KGP702
DMEM	Gibco	Cat.C11995500BT
fetal bovine serum	Sciencell	Cat.0500
TRIzol	Invitrogen	Cat.15596026
RIPA lysis buffer	KeyGEN	Cat.KGP702
SDS-PAGE	Epizyme Biotech	Cat.PG113
PVDF	Beyotime	Cat.FFP39
Triton X-100	Byeotime	Cat.P0096-100mL
Matrigel	BD Biosciences	Cat.356255
Critical commercial assays		
Superscript Reverse Transcriptase	Applied Biosystems	Cat.18080093
SYBR Green Master Mix	Applied Biosystems	Cat.A25741
Bicinchoninic Acid Protein Assay Kit	Beyotime	Cat.P0009
BeyoClick™ EdU Cell Proliferation Kit	Byeotime	Cat.C0075L
luciferase reporter vector	Promega	Cat.E1761
nucleotide circular single stranded scaffold DNA	New England Biolabs	Cat.N4040S
Experimental models: Cell lines		
NHAs	Procell	Cat.CP-H122
U118	Procell	Cat.CL-0458
A172	Procell	Cat.CL-0012
T98G	Procell	Cat.CL-0583
LN229	Procell	Cat.CL-0578
U251	Procell	Cat.CL-0237
THP-1	Procell	Cat.CL-0233
Experimental models: Organisms/strains		
BALb/c mice	Gempharmatech	N/A

(*Continued on next page*)

Continued

REAGENT or RESOURCE	SOURCE	IDENTIFIER
Oligonucleotides		
Primer: GAPDH-R (5′-3′)	GGCATGGACTGTGGTCATGAG	N/A
Primer: GAPDH-F (5′-3′)	TGCACCACCAACTGCTTAGC	N/A
Primer: TBX15-R (5′-3′)	GCACAGGGGAATCAGCATTG	N/A
Primer: TBX15-F (5′-3′)	AAAGCAGGCAGGAGGATGTT	N/A
Primer: TXNDC15-R (5′-3′)	GCGCGAAGAACATGACGAAG	N/A
Primer: TXNDC15-F (5′-3′)	CGCACAGCAAGCACCTGTA	N/A
Software and algorithms		
Grpahpad Prism v9.0	GraphPad software	N/A

RESOURCE AVAILABILITY

Lead contact

Further information and requests for resources and reagents should be directed to and will be fulfilled by the lead contact, Jun Dong (dongjun@suda.edu.cn).

Materials availability

All unique/stable reagents generated in this study are available from the lead contact with a completed Materials Transfer Agreement.

Data and code availability

This paper does not report any original code.

The data reported in this paper will be shared by the lead contact upon reasonable request.

Any additional information required to reanalyze the data reported in this paper is available from the lead contact upon reasonable request.

EXPERIMENTAL MODEL AND STUDY PARTICIPANT DETAILS

Patients and specimens

Glioma specimens (n = 50) and paired PTTs were obtained from the Department of Neurosurgery, Second Affiliated Hospital of Soochow University. The tissues were quickly placed in a solution (RNAlater, Thermo Fisher, Cat.AM7020) that preserves RNA and then stored at a very low temperature (−195.8°C) in liquid nitrogen. All patients are required to sign the informed consent. The relationship between clinical characteristics and TBX15 expression was shown in Table S1.

Animal studies

The animal experiments were approved by Institutional Animal Care and Use Committee of the Soochow University. The procedure was performed according to institutional ethics guidelines for animal experiments and National Institute of Health Principles. Four-weeks-old male BALb/c mice were purchased from Gempharmatech (Nanjing, China). After anesthetizing with 0.3% pentobarbital sodium via intraperitoneal injection, 5×10^4 LN229-Luci cells were injected into the right caudate nucleus of mice. The tumor growth was monitored using a live imaging system. The administration of nanoparticles was conducted via intravenous injection through the tail vein, on days 12, 14 and 16 of tumor modeling. Intracranial tumor size was measured at the indicated time points.

Ethics approval and consent to participate

This study was approved by the Research Ethics Committee of the Second Affiliated Hospital of Soochow University. All patients provided written informed consent.

Consent for publication

Written informed consent for publication was obtained from all the participants.

METHOD DETAILS

Data collection

To investigate the expression and clinical relation of TBX15/TXNDC5 in glioma, transcriptome data and clinical information of glioma patients were obtained from TCGA database and CGGA database. Related bioinformation data were obtained publicly.

Survival analysis

The median expression value of a gene was utilized as the threshold to partition the samples into high and low expression groups for the purpose of assessing survival distributions. Statistical analyses were conducted using R (version 4.2.1, https://www.r-project.org/). Kaplan-Meier survival curves were generated to visually represent overall survival, employing the 'survival' and 'survminer' packages within R.

Immune cell infiltration analysis

In order to assess disparities in immune cell infiltration, the samples were categorized into high and low expression groups according to the median gene expression value. The CIBERSORTx algorithm (https://cibersortx.stanford.edu/) was employed to estimate the relative infiltration of 22 distinct immune cell types within each group.

Cell culture and transfection

We obtained normal human astrocytes together with human glioma cell lines (U118, A172, T98G, LN229 and U251) from Procell (Wuhan, China). All cells were cultured in Dulbecco's modified Eagle medium (DMEM, Cat.C11995500BT, Gibco, USA) supplemented with 10% fetal bovine serum (FBS, Cat.0500, Sciencell, USA) in a 5% CO_2 incubator at 37°C. The cells were passaged once the 80% confluent.

The vectors and related compounds used for transfection were from GenePharma (Shanghai, China). The cells were placed into a six-well plate and allowed to grow until they reached 90% confluent, and transfected with lentiviruses expressing shRNAs, overexpression plasmids or corresponding negative controls according to the instructions provided by the manufacturer.

Quantitative reverse transcription-polymerase CHAIN reaction

Total RNA was extracted using TRIzol (Cat.15596026, Invitrogen, USA) and quantified. Equal amounts of RNA per sample were reverse transcribed into complementary DNA (cDNA) using Superscript Reverse Transcriptase (Cat.18080093, Applied Biosystems, USA). Besides, qRT-PCR was conducted on the ABI 7500 real-time PCR system (Applied Biosystems, USA) using SYBR Green Master Mix (Cat.A25741, Applied Biosystems, USA). Glyceraldehyde 3-phosphate dehydrogenase (GAPDH) was utilized as the internal control.[33]

Western blotting

Protein was extracted from tissues and cells using the RIPA lysis buffer (Cat.KGP702, KeyGEN, China) and quantified using the Bicinchoninic Acid Protein Assay Kit (Cat.P0009, Beyotime, Shanghai, China). Equal amounts of protein were isolated from each sample and separated using 12% sodium dodecyl sulfate polyacrylamide gel electrophoresis (SDS-PAGE, Cat.PG113, Epizyme Biotech, Shanghai, China). The separated proteins were then transferred onto polyvinylidene fluoride (PVDF, Cat.FFP39, Beyotime, Shanghai, China) membranes for further analysis. Following the blocking of membranes with 5% skim milk, the membranes were incubated overnight at 4°C with rabbit anti-TBX15 (Cat.25148-1-AP, Proteintech, USA), rabbit anti-TXNDC5 (Cat.19834-1-AP, Proteintech, USA) and rabbit anti-GAPDH (Cat.60004-1-Ig, Proteintech, USA) antibodies. Thereafter, the membranes were further incubated with HRP-conjugated conjugated goat anti-rabbit/mouse IgG (H + L) (Cat.SA00001-2/SA00001-1, Proteintech, USA) for 2 h. To visualize the protein bands, a chemiluminescence reagent was used in conjunction with Tanon 4600SF (Tanon, China).[34]

EdU assay

The working solution of 20 μM Alexa Fluor 555-EdU was prepared following the instructions of the BeyoClick EdU Cell Proliferation Kit (Cat.C0075L, Byeotime, Shanghai, China). The cells were incubated with EdU for 1 h, fixed by 4% paraformaldehyde for 20 min and washed thrice with PBS containing 3% BSA. After permeabilizing with 0.1% Triton X-100 (Cat.P0096-100mL, Byeotime, Shanghai, China) for 20 min, the cells were incubated with Click-iT EDU mixture for 30 min. The cells were then counterstained with Hoechst33342 solution for 5 min in the dark, and observed under a fluorescence microscope (Olympus, Japan).[35]

Transwell assay

The cells were seeded into the upper chambers of transwell inserts at the density of 3×10^4 cells/well in serum-free DMEM, and the lower chambers were filled with 600 μL complete medium. Following a 48-h incubation period, the chambers were washed thrice with distilled water. Subsequently, the cells were subjected to fixation with methanol for a duration of 20 min, followed by staining with 1% crystal violet for 30 min. The dye was rinsed with distilled water, and the migrating/invading cells were counted with a light microscope (Olympus, Japan) and ImageJ software. To conduct the invasion assay, the upper chambers of the cell culture apparatus were precoated with Matrigel (Cat.356255, BD, USA).[36]

Co-culture model

For transwell assay, PMA-stimulated THP-1 cells were added into the upper chamber (8 μm, Corning, NY, USA) and A172/LN229 were plated into the lower chamber. 48 h later, THP-1 cells (macrophages) remaining in the upper chamber were removed and the migrated THP-1 cells (macrophages) were fixed, stained, and captured using a microscope.

For polarization detection, A172/LN229 were added into the upper chamber (0.4 μm, Corning, NY, USA) and PMA-stimulated THP-1 cells (macrophages) were plated into the lower. After co-culture for 48 h, THP-1 cellular polarization was detected by flow cytometry.

Flow cytometry

THP-1 derived cells were harvested, washed thrice with PBS and then incubated with anti-CD68 (Cat.333813, Biolegend, USA) and anti-CD163 (Cat.333605, Biolegend, USA) antibodies for a duration of 20 min under dark conditions. Following this incubation, the cells were rinsed thrice with PBS and acquired on the Agilent Navocyte flow cytometer, and analyzed with FlowJo.

Luciferase reporter assay

The TBX15 binding sites in the TXNDC5 promoter sequence underwent amplification or mutagenesis, which were subsequently cloned into luciferase reporter vector (Cat.E1761, Promega, USA). Following transfection with the WT (P) or mutated (P1, P2 and P3) luciferase reporter vector along with either the TBX15 overexpression or control plasmid, glioma cells were subjected to a 48-h incubation period. The relative luciferase activity was subsequently measured using the Dual-Glo Luciferase Reporter Assay System (Promega, USA).

Immunohistochemistry (IHC)

The paraffin-embedded tissues were sectioned into 6 μm-thick slices and blocked with 5% normal goat serum, followed by the incubation overnight with rabbit anti-TBX15 (Cat.PA5-36143, Invitrogen, USA) and rabbit anti-TXNDC5 (Cat.PA5-83240, Invitrogen, USA) antibodies at 4°C. The following day, the sections were incubated with corresponding secondary antibodies for 1 h at room temperature. After developing the color with DAB substrate, the sections were counterstained with hematoxylin, followed by dehydration, clarification, and mounting for further analysis. Finally, the images were obtained under a microscope (Olympus, Japan).[37]

Synthesis of nanoplatform

TDONs were constructed as described previously. Briefly, a 7249-nucleotide circular single stranded scaffold DNA (M13mp18, 10nM, Cat.N4040S, New England Biolabs, England), staple strands (50nM each), and capture strands for FAoligo hybridization (50nM each) were mixed in 1× TAE/Mg^{2+} buffer. The mixture was subjected to annealing in a PCR thermocycler, with a gradual decrease in temperature from 90°C to 4°C at the rate of 1°C per 5 min. The resulting product was washed with 1×TAE-Mg^{2+} buffer, and subsequently filtered through AmiconUltra centrifugal filters (100 kDa) at 6000 rpm for 10 min to remove any excess staple strands. The capture strands that protruded from the purified tDONs were deliberately synthesized to be complementary to shRNA-oligo, sh-TBX15-oligo and RGB-oligo. The shRNA-tDONs were assembled by annealing shRNA-oligo and RGB-oligo (1.8 μM, 5 times excess) with purified tDONs (10 nM) through a gradual temperature reduction 37°C–4°C using a PCR thermocycler. Similarly, Sh-TBX15-tDONs were assembled by annealing sh-TBX15-oligo and RGB-oligo (1.80 μM, 5 times excess) with purified tDONs (10 nM) through the same gradual temperature reduction process. To eliminate any surplus shRNA-oligo, sh-TBX15-oligo or RGB-oligo, the synthetic nanomedicines were subjected to washing with 1× TAE-Mg^{2+} buffer, followed by filtration using AmiconUltra centrifugal filters (100 kDa) at 6000 rpm for 10 min.[20]

QUANTIFICATION AND STATISTICAL ANALYSIS

Data were presented as the mean ± standard deviation (SD). Data comparison of two groups was carried out by Student's *t* test. Multi-factorial comparisons were carried out by two-way ANOVA. The data about immunoinfiltration was analyzed by CIBERSORTx algorithm. The correlation analysis was confirmed by Pearson's correlation. The graphs were plotted using the GraphPad Prism 9.0 software (GraphPad Software, CA, USA). *p* value less than 0.05 was indicative for the statistical significance.